Science of the Total Environment 951 (2024) 175812

Contents lists available at ScienceDirect

Science of the Total Environment

journal homepage: www.elsevier.com/locate/scitotenv

Enhancing biofilm formation with powder carriers for efficient nitrogen and phosphorus removal

Yi Yang [a,b], Yuting Zhu [c], Defu Gan [a,b], Xiang Cai [d], Xiaodi Li [a,b], Xinchao Liu [c], Siqing Xia [a,b,*]

[a] State Key Laboratory of Pollution Control and Resource Reuse, College of Environmental Science and Engineering, Tongji University, Shanghai 200092, China
[b] Shanghai Institute of Pollution Control and Ecological Security, Shanghai 200092, China
[c] Tongji Architectural Design (Group) Co., Ltd., Shanghai 200092, China
[d] College of Geography and Environmental Sciences, Zhejiang Normal University, Jinhua 321004, China

HIGHLIGHTS

- Integrating powder carriers into activated sludge enhances the removal of N and P.
- The extended DLVO theory was applied to describe the sludge aggregation properties.
- Powder carriers have high biomass immobilizatsion ability.
- The system was overwhelmingly dominated by *Candidatus_Competibacter* (10.46–13.18 %).

GRAPHICAL ABSTRACT

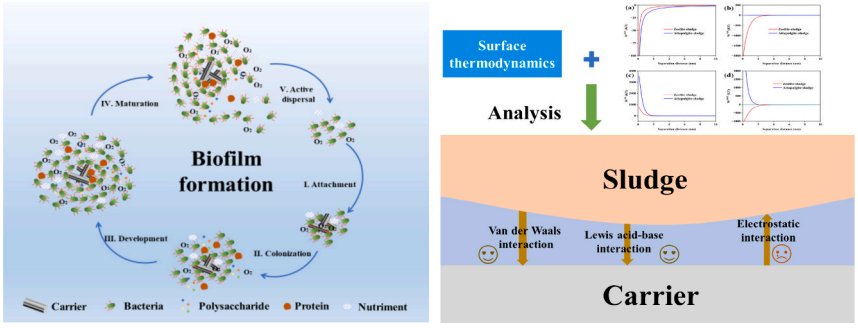

ARTICLE INFO

Editor: Yifeng Zhang

Keywords:
Powder carriers
Wastewater treatment
Microbial community
Mechanism of biofilm formation

ABSTRACT

This study assesses the improvement in nitrogen and phosphorus removal from wastewater achieved through the integration of zeolite and attapulgite carrier materials into the activated sludge (AS) process. It was found that the addition of these materials significantly enhanced the processing performance of the reactor. Specifically, the use of zeolite and attapulgite powders increased sludge particle sizes to averages of 231.56 μm and 219.62 μm, respectively. This facilitated micro-granule formation, substantially improving the settling characteristics of the sludge and boosting the activity and proliferation of essential microbes. Illumina MiSeq sequencing demonstrated significant accumulations of DGAOs (*Candidatus_Competibacter*) and DPAOs (*Candidatus_Accumulibacter*). Furthermore, these carriers augmented the protein content in extracellular polymers, enhancing the hydrophobicity of the sludge and promoting aggregation. Comparative analysis based on the extended Derjaguin, Landau, Verwey, and Overbeek (DLVO) theory indicated a preferential adhesion affinity of sludge for zeolite compared to attapulgite, attributed primarily to Lewis acid-base and electric double-layer interactions. These findings underscore zeolite's enhanced efficacy in biomass fixation and suggest significant potential for the technological advancement of wastewater treatment plants.

* Corresponding author at: 1239 Siping Road, Shanghai 200092, China.
E-mail address: siqingxia@tongji.edu.cn (S. Xia).

https://doi.org/10.1016/j.scitotenv.2024.175812
Received 13 June 2024; Received in revised form 13 August 2024; Accepted 24 August 2024
Available online 26 August 2024

1. Introduction

The rapid industrialization and rising living standards have increased wastewater discharge, posing significant challenges to the aquatic environment (Ruprecht et al., 2021; Sun et al., 2016). Untreated or inadequately treated wastewater contributes to eutrophication, endangers aquatic life, and disrupts the biogeochemical cycles of nitrogen (N) and phosphorus (P), increasing mortality rates (Powley et al., 2016). Traditional wastewater treatment plants (WWTPs), primarily designed to remove organic matter and suspended solids, are increasingly inadequate, particularly in regions vulnerable to nutrient pollution (Hasan et al., 2021; Qu et al., 2022). Consequently, the development of effective treatment methods to reduce nutrient levels has become a global environmental priority.

Biofilm systems, including moving bed biofilm reactors (MBBRs) and fixed bed biofilm reactors (FBBRs), are emerging as effective alternatives (Abu Bakar et al., 2018; Osama et al., 2023). These systems offer numerous benefits over conventional activated sludge processes, such as lower sludge production, shorter hydraulic retention times, reduced spatial requirements, higher concentrations of mixed liquid volatile suspended solids (MLVSS), and enhanced stability (Arabgol et al., 2022; Osmani et al., 2021). Biofilm communities in these systems also tend to be more diverse than those in traditional activated sludge setups (Lago et al., 2024; Wolff et al., 2021). MBBRs function effectively under both anaerobic/anoxic and aerobic conditions (Wang et al., 2023b). In aerobic settings, which typically involve nitrification and chemical oxygen demand (COD)/biochemical oxygen demand (BOD) removal, the aeration supplied often exceeds the dissolved oxygen (DO) requirements for microbial activity, thus increasing operating costs (Collivignarelli et al., 2019; Gupta et al., 2022). Conversely, anaerobic/anoxic systems rely on mechanical mixing, presenting challenges in achieving efficient mixing, especially during the initial biofilm formation stages (Matheus et al., 2021). Initially, biocarriers are buoyant due to their low density, but as biofilms develop and microbes colonize the carriers, the density increases, enhancing mixing capabilities (Arabgol et al., 2022; Aslam et al., 2024). However, suboptimal airflow patterns can still create stagnant areas. Recent studies highlight that smaller carrier sizes and increased specific surface areas enhance microbial adhesion and reduce biofilm colonization cycles, thereby boosting system efficiency (Wang et al., 2024b). Additionally, powdered carriers, which are smaller and require less energy for fluidization compared to traditional centimeter-sized suspension carriers, have proven more effective. Research indicates that incorporating zeolite, diatomite, activated carbon, and attapulgite into sludge systems significantly improves the removal efficiency of COD and nutrients (Jiang et al., 2019; Park et al., 2003; Wang et al., 2024a). For example, Wang et al. demonstrated that using diatomite as a carrier, enhances sludge sedimentation and prevents swelling (Wang et al., 2024b). Mu et al. showed that adding powder carriers increases the total phosphorus removal rate by 15.73 % and improves the anaerobic phosphorus release capacity of activated sludge (Mu et al., 2023). While these studies offer valuable insights into the enhancement of biological water treatment, including the analysis of sludge physicochemical properties and microbial community composition with the addition of carriers, there remains a significant research gap concerning the thermodynamics of carrier-sludge interface aggregation. Understanding the thermodynamic mechanisms governing this interface is crucial for exploring biofilm formation (Fan et al., 2021; Zhao et al., 2022). Therefore, it is essential to integrate treatment effeciency, component analysis, thermodynamic studies, and microbial community analysis to thoroughly investigate the comprehensive mechanisms that drive the efficacy of powder carrier systems in enhancing wastewater treatment.

Zeolite and attapulgite have densities similar to that of water, which allows these carriers to be effectively distributed in sewage. Additionally, their high biocompatibility and porous nature create favorable conditions for the adhesion and growth of microorganisms (Chen et al., 2023; Sakaveli et al., 2023; Wang et al., 2020). In this study, zeolite and attapulgite were selected as representatives of powdered carriers (PC), and three reactors were established to treat simulated domestic sewage. The impact of these carriers on denitrification and phosphorus removal was assessed through water quality monitoring. Additionally, the role of extracellular polymeric substances (EPS) in the formation of micro-granular sludge was explored. The extended DLVO theory was applied to elucidate the interactions between the carriers and sludge. Microbial sequencing technology was employed to investigate the effects of the carriers on microbial community dynamics. Collectively, these approaches provided new insights into advancing wastewater treatment technologies.

2. Materials and methods

2.1. Experimental setup

Sludge for this experiment was sourced from the second sedimentation tank of a Shanghai wastewater treatment plant (WWTP). The initial mixed liquid suspended solids (MLSS) concentration in each reactor was approximately 3500 mg/L, with a working volume of 4 L. The influent ratio, defined as the ratio of influent to working volume, was set at 50 %. On the first day of operation, reactors S2 and S3 received 4 g/L of powdered zeolite and attapulgite, respectively. The zeolite and attapulgite powder carriers were filtered through a 47–74 μm screen before use (Figs. S2 and S4). The specific surface areas of zeolite and attapulgite are 22.84 m^2/g and 30.61 m^2/g, respectively. Reactor S1 served as the control in the blank group. The sludge retention time (SRT) was consistently maintained at 30 days. To offset carrier loss during sludge discharge, the concentration of carrier was kept constant at 4 g/L through daily quantitative additions (refer to Text S1). The dissolved oxygen (DO) level in the aeration segment was controlled between 2 and 4 mg/L, and the system was operated at room temperature (25 °C). The experiment lasted 90 days and was conducted in two distinct phases, operating continuously in the anoxic/oxic/anoxic (AOA) mode. Further details are available in Fig. 1 and Table 1 of the main document. For information on the composition of the synthetic wastewater used, please refer to the supplementary materials, Tables S1 and S2.

2.2. Analytical methods

Daily influent and effluent water samples from the reactor were collected and filtered through a 0.45 μm membrane for subsequent analysis. Wastewater parameters including chemical oxygen demand (COD), ammonia nitrogen (NH_4^+-N), nitrate nitrogen (NO_3^--N), total nitrogen (TN), and total phosphorus (TP), along with activated sludge characteristics such as mixed liquor suspended solids (MLSS), mixed liquor volatile suspended solids (MLVSS), and 5-min settling velocity (SV5) were determined using standard methods (APHA, 2012). The pH and DO levels of the wastewater were measured with a pH meter and a dissolved oxygen meter, respectively. The particle size distribution of the sludge was assessed using a laser particle size analyzer, covering a size range from 0.01 to 2000 μm. The sludge samples collected at the end of the long-term test described in Section 2.1 were subjected to sludge morphology analysis. Zeolite and attapulgite samples were magnetically stirred in a 0.4 % (*w/v*) water solution at 500 rpm for 60 min. A contact angle analyzer was used to measure the contact angles of the samples with water, glycerol, and diiodomethane, with averages calculated from all observations. Additionally, the zeta potential of the sludge, zeolite, and attapulgite was measured in a room-temperature 0.1 M NaCl solution. Detailed information regarding their characterization is provided in the Supplementary Information (Text S2).

2.3. EPS extraction and analysis

The mixed liquor was sampled from the bioreactor every ten days. To extract EPS, the heating method was applied. The phenol-sulfuric acid method was used to quantify the amount of polysaccharide (PS), and a modified Lowry colorimetric approach was used to measure the amount of PN (Tang et al., 2020). All measurements were conducted in triplicate. The detailed descriptions are provided in the Supplementary Information (Text S3).

2.4. Surface thermodynamics and extended DLVO theory

In microbial populations, biofilms primarily consist of bacterial cells, which range in size from approximately 0.5 to 2 μm, similar to colloidal particles. Consequently, the process of bacterial fixation aligns well with the principles of DLVO theory (Bos et al., 1999). The interfacial free energy (ΔG_{adh}) between bacteria and water is composed of two components: the van der Waals interaction free energy (ΔG_{adh}^{LW}) and the Lewis acid-base interaction free energy (ΔG_{adh}^{AB}) (Li et al., 2023). In terms of thermodynamics, when $\Delta G_{adh} < 0$, microorganisms spontaneously adhere to the surface of the carrier; otherwise, adhesion does not occur.

Acknowledging this, Van Oss proposed an extended DLVO theory that integrates surface thermodynamics with the classical DLVO theory, encompassing the Lifshitz-van der Waals force (W^{LW}), the electrostatic force (W^{EL}), and the Lewis-acid base force (W^{AB}). The total interaction energy (W^{ToT}) can be expressed as a function of the separation distance (h). The utilizes surface thermodynamic calculations to compute W^{LW}, W^{EL}, and W^{AB} (Xu et al., 2016). Notably, due to the substantial difference in size between mineral particles and bacteria, the former is treated as infinitely thick plates, while the latter is approximated as spheres. The calculations for these components follow the formulas detailed in the study. For a comprehensive understanding of the intricacies involved in the calculation process, please refer to the detailed descriptions provided in the Supplementary Information (Text S4).

2.5. DNA extraction and high-throughput sequencing data analysis

At the end of the long-term test, the activated sludge samples were analyzed at Shanghai Majorbio Bio-pharm Technology Co., Ltd. The analysis involved agarose gel electrophoresis detection, PCR amplification, purification of the amplification product, and sequencing of the 16S rRNA gene. The amplified fragment had a length of 468 bp, and the primer used was 338F_806R. Details of the materials and methods for microbiological analysis are provided in the Supporting Information (Text S5). Raw data has been deposited to the NCBI (PRJNA1143701).

Table 1
The operational conditions during the whole experiment.

Periods	Phase I	Phase II
Duration (d)	1–45	46–90
OLR (kg COD/m^3/d)	0.733	0.923
NLR (g N/L/d)	0.113	0.147

3. Results and discussion

3.1. Performance of the reactor

The effluent concentrations and removal rates of COD, nitrogen, and phosphorus throughout the operation of the three reactors are shown in Figs. 2 and S1, respectively. After a 15-day adaptation period in phase I, the effluent COD concentration of all three reactor groups was maintained below 30 mg/L. However, during phase II, as the organic loading rate (OLR) increased to 0.923 kg COD/m^3/d, there was a temporary rise in COD effluent concentration. Notably, reactors S2 and S3 exhibited significantly higher COD removal efficiency during the long-term testing period.

In phase I, after a 16-day adaptation period, the NH_4^+-N concentration in S2 was lower than 1 mg/L. S3 required an additional 20 days of adaptation for the effluent NH_4^+-N concentration to drop below 1 mg/L. However, during phase II, as the nitrogen loading rate (NLR) increased to 0.147 g N/L/d, there was a temporary rise in NH_4^+-N effluent concentration. After achieving stable operation, the ammonia nitrogen effluent concentrations for S1, S2, and S3 were 1.01 ± 0.32 mg/L, 0.84 ± 0.25 mg/L, and 0.92 ± 0.14 mg/L, respectively. Nitrogen removal in wastewater treatment involves two stages: nitrification and denitrification. The primary factor leading to substandard TN concentration in the effluent is low denitrification efficiency. During the initial stage of operation, the higher NO_3^--N effluent concentration was attributed to the need for activated sludge to adapt to environmental changes and the time required for microorganism growth on the carrier. Following stable operation (30–45 days), the nitrate concentrations for S1, S2, and S3 were 10.67 ± 1.09 mg/L, 6.51 ± 0.77 mg/L, and 7.96 ± 1.35 mg/L, respectively. During Phase II, with increased NLR, all reactors experienced fluctuations, with S1 showing a larger amplitude. This indicates that adding carriers can enhance the reactor's resistance to variations in water quality. The reactors achieved stable operation on the 60th day, with nitrate concentrations in the effluent at 12.65 ± 1.23 mg/L, 9.24 ± 1.26 mg/L, and 8.83 ± 1.69 mg/L, respectively. Ultimately, the final TN removal rates for the three reactor groups were 88.49 ± 1.98 %, 88.10 ± 1.50 %, and 83.85 ± 1.51 %.

In this work, we evaluated not only the removal performance of nitrogen but also the removal performance of phosphorus. Generally, phosphorus removal requires a shorter SRT, while nitrogen removal requires a longer SRT. Despite this contradiction, we designed an

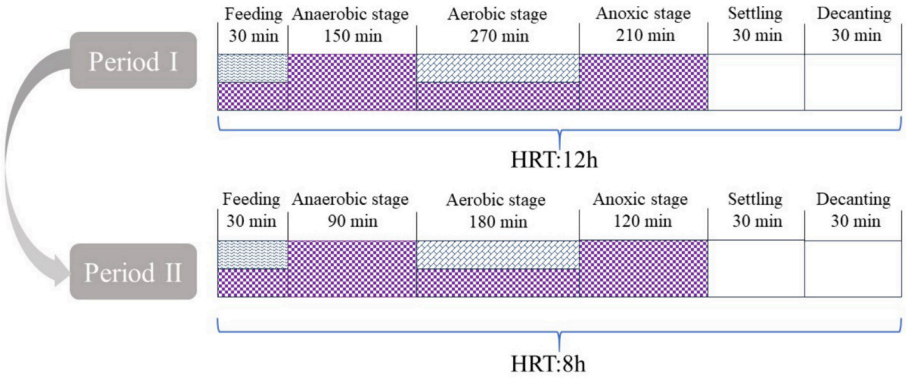

Fig. 1. The operation mode of the reactor.

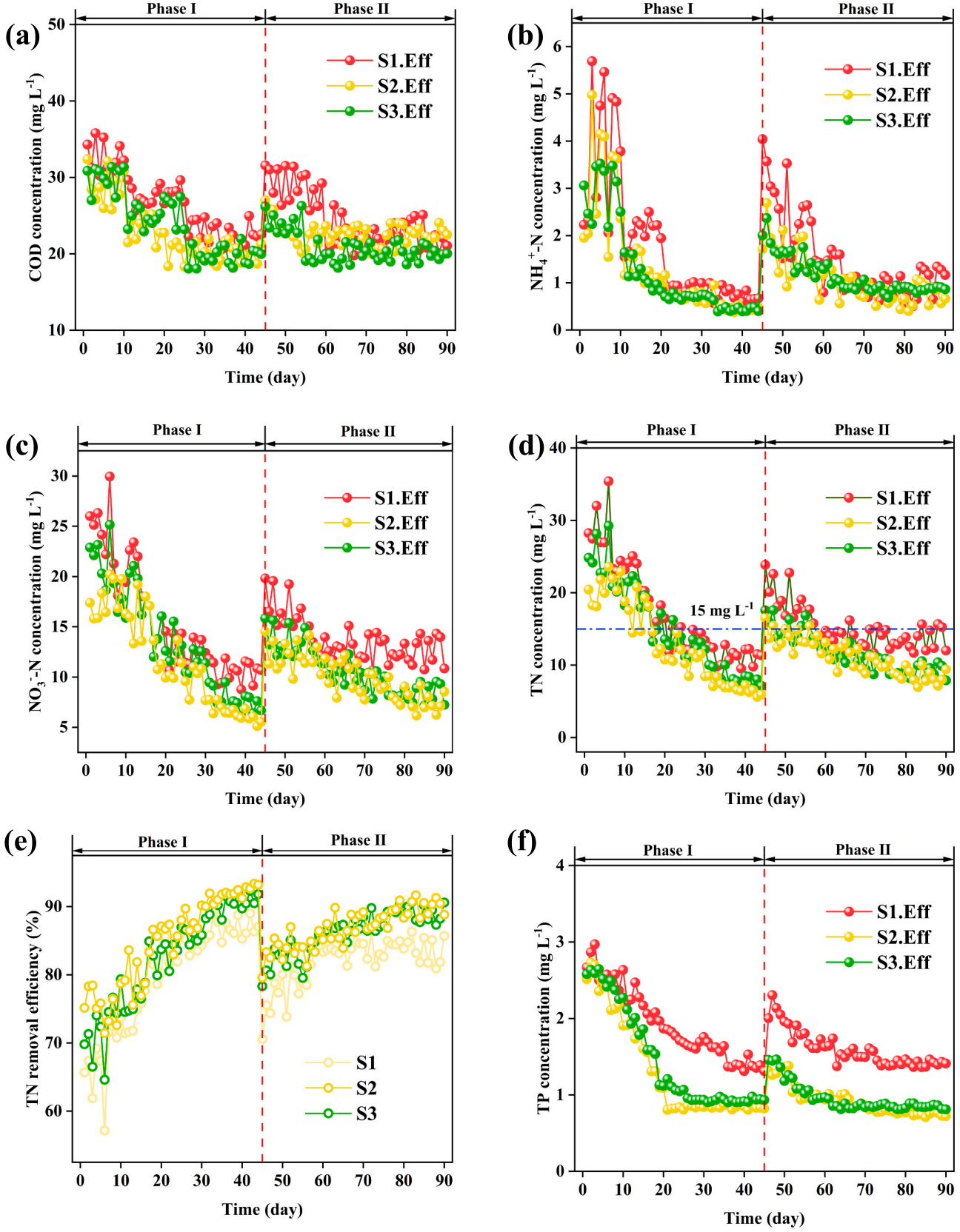

Fig. 2. Performance of the reactors during 90 days of operation. (a) the effluent qualities of COD (b) the effluent qualities of NH_4^+-N; (c) the effluent qualities of NO_3^--N; (d) the effluent qualities of TN; (e) the removal efficiency of TN; (f) the effluent qualities of TP.

experiment with a longer SRT (30 days) and still achieved excellent phosphorus removal performance. The influent TP concentration was 6.5 mg/L. The effluent quality must comply with Grade A effluent standards for municipal sewage treatment plants (GB 18918–2002, Table S3), which stipulates that the TP concentration should be <0.5 mg/L. The effluent TP concentrations in the three reactor groups were 1.44 ± 0.06 mg/L, 0.78 ± 0.04 mg/L, and 0.85 ± 0.02 mg/L, respectively. The TP removal rates for the three reactor groups were 77.95 ± 0.96 %, 88.15 ± 0.54 %, and 86.94 ± 0.37 %, respectively. Although the effluent concentration of TP did not meet the 0.5 mg/L requirement stipulated by the sewage discharge standard, the lower TP effluent concentration can significantly reduce the usage of chemical agents in the subsequent chemical phosphorus removal process.

3.2. Morphology and composition analysis of sludge

The formation process of microbial adhesion on powder carriers was examined using SEM. During the granulation process, sludge flocs gradually disappeared, and EPS wrapped around the surface of the carrier, forming a smooth biofilm (Fig. 3). With the proliferation of microorganisms, a large number of bacilli and globular bacteria appeared on the surface of the carriers. The powder carriers added to the reactor were buried in the sludge, promoting granulation and enhancing the structural stability of the micro-granular sludge. In contrast, the activated sludge system without the carrier had more filamentous bacteria.

When the total SRTs were the same, adding the carriers significantly increased the biomass MLVSS in the reactor. Compared with S1, the biomass MLVSS of S2 and S3 increased steadily throughout the reactor operation. After 90 days, the MLVSS of the three reactors stabilized at approximately 2471.93 mg/L, 3786.73 mg/L, and 3458.59 mg/L, respectively. To further study microbial activity, the specific oxygen uptake rate (SOUR) was determined, as SOUR is a key indicator of microbial metabolic activity in sludge (Chen et al., 2017). After 90 days of operation, the SOUR values of the three reactors were 0.19, 0.22, and 0.20 mg O_2/(mg VSS·h), respectively. The evidence indicates that adding carriers can increase the amount of microorganisms, without affecting their activity. The settling performance of activated sludge was further studied, and SV5 was measured, as shown in Fig. 4a. Although the concentration of activated sludge increased, its settling property was not affected. Notably, the addition of carriers in S2 and S3 resulted in better sedimentation performance compared to S1. After 90 days of operation, the particle size of activated sludge increased from 86.38 μm to 131.46 μm in S1, 231.56 μm in S2, and 219.62 μm in S3. The larger particle size of activated sludge in the reactor with zeolite (S2) indicates that the biofilm formed is more prone to stratification, creating anoxic and anaerobic zones inside the biofilm, which is beneficial for nitrogen removal. This phenomenon aligns with the superior nitrogen removal performance of S2, which also showed stronger impact resistance and more stable operation. The S3 reactor demonstrated that adding attapulgite also increased the particle size of activated sludge, aiding in improving the reactor's denitrification performance. Overall, the addition of carriers improved the sedimentation performance of reactor-activated sludge and helped mitigate sludge swelling. This improvement is primarily due to the increase in the particle size of the activated sludge. According to Stokes law, the sedimentation rate is proportional to the square of the particle size of the activated sludge (Iritani et al., 2015). Additionally, the carrier acts as a flocculant, accelerating the settling of activated sludge through adsorption bridging, net trapping, and other mechanisms (Zhang et al., 2023).

3.3. Effects of carriers on EPS secretion

EPS, metabolic products accumulating on bacterial cell surfaces, are crucial for forming and stabilizing biofilms. After 90 days of operation, the total EPS content in the three reactor groups measured 344.03 ± 17.20, 392.46 ± 19.62, and 356.67 ± 17.83 mg/g VSS, with PN/PS ratios of 2.82 ± 0.02, 3.02 ± 0.03, and 2.94 ± 0.03, respectively (Fig. 5a). Analysis showed significantly higher EPS content in S2 and S3 compared to S1, indicating that PN and PS in EPS play a key role in microbial agglomeration. Certain base groups in EPS proteins, such as alanine and cysteine carry positive charges and exhibit hydrophobic effects, reducing the surface potential of the micro-biomass and promoting agglomeration (Xiao et al., 2021; Yang et al., 2024a). A higher PN/PS ratio in EPS typically indicates stronger hydrophobicity and more adsorption sites (Zhang et al., 2018). Notably, the PN content and PN/PS ratio of S2 are significantly higher than those of S1 and S3, indicating that the zeolite carrier has a stronger microbial agglomeration ability (Fig. 5b). This finding is consistent with the largest sludge particle size observed in S2. Metal ions can impact microorganism adhesion by affecting EPS and sludge hydrophobicity. Zeolite and attapulgite, rich in Mg and Si elements, benefit bacterial EPS formation, enhancing adsorption and binding energy with carriers (Li et al., 2023).

3.4. The interaction between carrier and sludge

Choosing the right biofilm carrier is crucial for effective wastewater treatment through biofilm processes, with the carrier's biocompatibility significantly enhancing efficiency. The stability of sludge results from the interaction between hydrophilicity, caused by water molecules or hydrophilic substances, and hydrophobicity generated by the aggregation of sludge cells and carrier particles (Fan et al., 2021). Hydrophobic interactions, which are long-range attractive forces between two hydrophobic surfaces, play a crucial role in bacterial adsorption. Contact angle measurements (see Table 2) between zeolite and sludge indicate that sludge exhibits higher hydrophobicity than zeolite, suggesting a potentially greater adsorption capability.

Incorporating surface thermodynamics and DLVO theory helps us understand how activated sludge microorganisms adhere to carriers like zeolite or attapulgite. From a thermodynamic viewpoint, a spontaneous

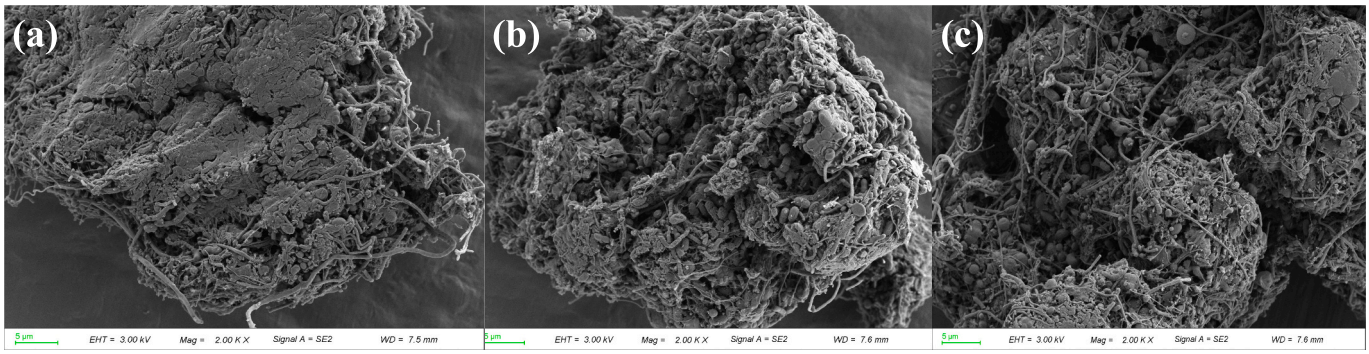

Fig. 3. The SEM images of sludge samples. (a) S1; (b) S2; (c) S3.

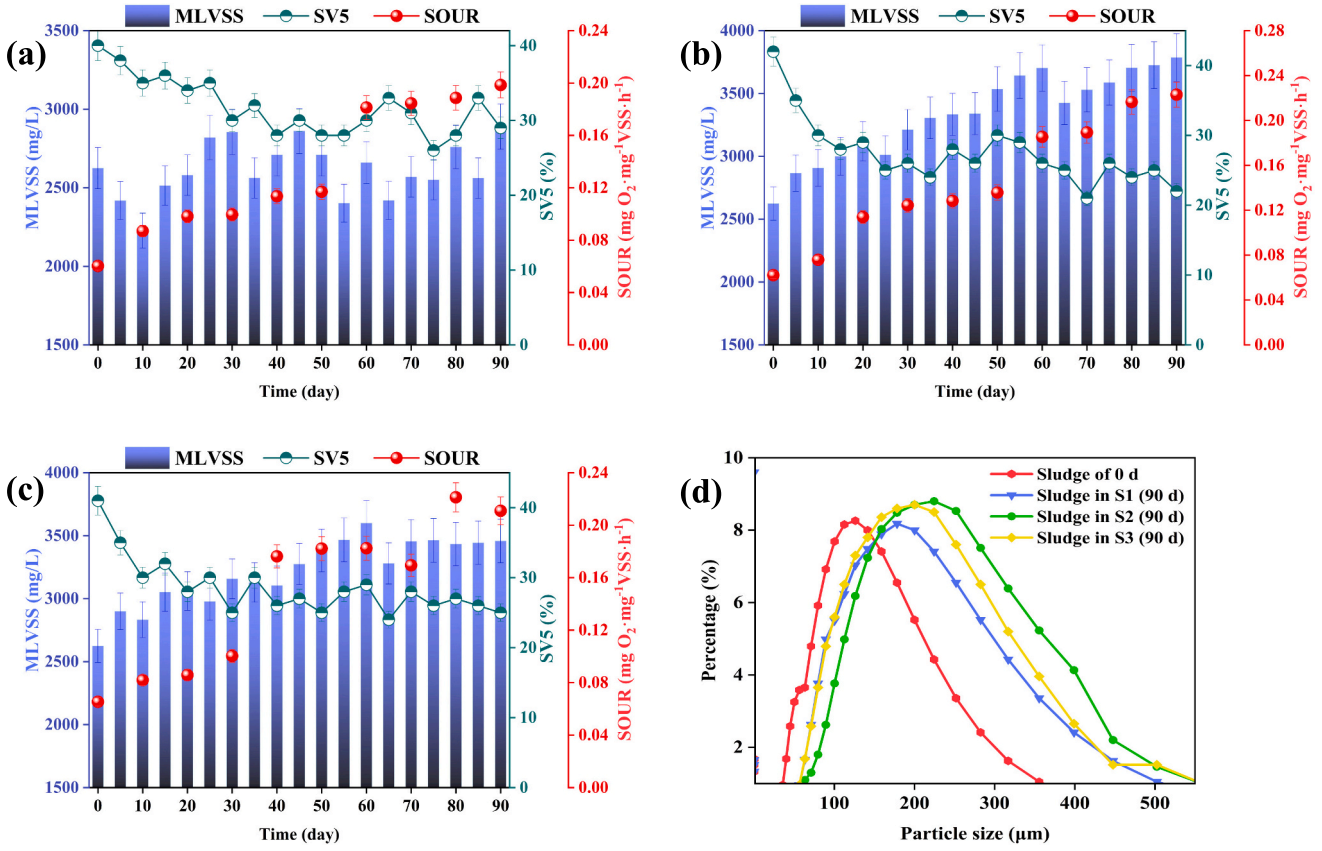

Fig. 4. Variations of the sludge characteristics during the experimental period: (a) MLVSS, SV5, and SOUR of the S1 reactors; (b) MLVSS, SV5, and SOUR of the S2 reactors; (c) MLVSS, SV5, and SOUR of the S3 reactors; (d) Sludge particle size.

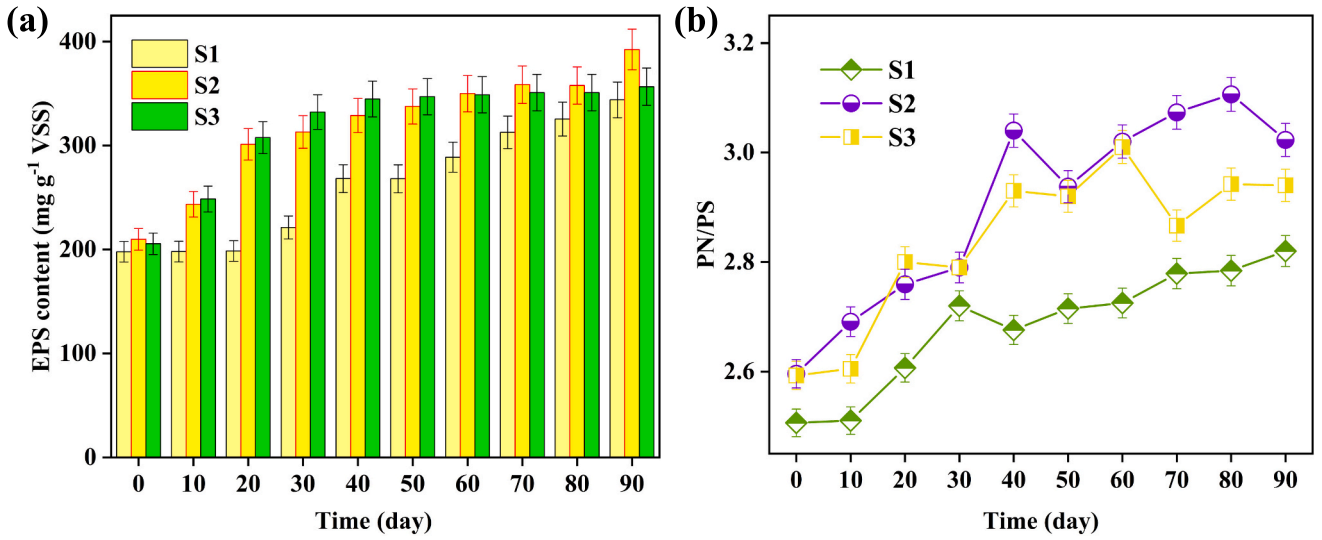

Fig. 5. (a) The EPS concentration; (b) the proteins to polysaccharides ratio on a weight basis.

Table 2
The contact angle and zeta potentials of sludge, zeolite, and attapulgite.

System	Water (°)	Propanetriol (°)	Diiodomethane (°)	Zeta (mV)
Sludge	34.99 ± 0.44	61.84 ± 0.25	32.56 ± 0.75	−9.91 ± 0.48
Zeolite	52.50 ± 0.64	82.54 ± 0.59	19.96 ± 0.52	−4.58 ± 0.51
Attapulgite	12.17 ± 0.43	67.17 ± 0.28	60.57 ± 0.48	−22.17 ± 0.63

reaction tends towards reduced free energy, leading to bacterial attachment when the surface free energy of sludge-carrier attachment turns negative. The surface free energy (ΔG_{adh}) for zeolite-sludge and attapulgite-sludge is −12.40 mJ/m^2 and −3.08 mJ/m^2, respectively, indicating a higher propensity for sludge to adsorb onto zeolite (refer to Table 3). It is worth noting that the ΔG_{adh}^{AB} of zeolite and activated sludge is −11.01 mJ/m^2, indicating that the Lewis acid-base interaction free energy plays a major role in the microbial agglomeration process. To delve into the initial adhesion behavior of sludge on carrier surfaces, we analyzed the interaction potential energy curve between sludge and zeolite or attapulgite carriers (refer to Fig. 6). At minimal distances between microorganisms and carriers, a maximum interaction energy barrier occurs (Zhang et al., 2019). Microorganisms can aggregate only after overcoming this barrier. Generally, when $W^{TOT} < 0$, the interaction force is attractive; otherwise, it is a repulsive force (Boks et al., 2008). The W^{TOT} at the closest contact distance with sludge, zeolite, and attapulgite (d = 0.158 nm) is negative: −1140 kT and 3254 kT, respectively. This suggests that microorganisms can readily overcome the energy barrier between zeolite carriers, forming tight aggregates. Both zeolite and attapulgite exhibit attractive van der Waals interactions, with attapulgite showing a stronger van der Waals interaction with sludge. The zeta potential on the surface of bacteria is also negative due to the presence of negatively charged functional groups, such as carboxylates in lipoproteins and lipopolysaccharides, on the cell walls under physiological conditions (Li et al., 2023). The zeta potentials of both zeolite and attapulgite surfaces are negative within the test range, but the repulsion between attapulgite and sludge is stronger. The interaction potential energy curve shows that the electrostatic interaction potential energy between the carrier and sludge remains greater than zero throughout the interaction distance (d = 0.158–10 nm), indicating a strong repulsive force, particularly with attapulgite carriers.

3.5. Dynamics of microbial ecology

3.5.1. Microbial diversity and richness

Table S4 presents the bacterial richness and diversity estimators obtained from sequencing analysis. The high coverage indices (0.9994–0.9999) indicate sufficient sampling depth to cover most species, as confirmed by the plateaued rarefaction curves (Fig. 7a), suggesting that the sequencing results accurately reflect microbial diversity (Ma et al., 2023). The α-diversity index shows a significant decrease in both community abundance and diversity in S1, S2, and S3 compared to the Seed sample. This decline is attributed to the enrichment of microorganisms adapted to the environmental conditions, leading to reduced diversity but increased abundance. S1 exhibited the highest sample richness indices (Ace and Chao), indicating greater species richness in the environment without carrier addition. However, the Shannon index of S2 and S3 (4.2739, 4.0799) was lower than that of the Seed sludge (5.0162) due to carrier addition. The decrease in microbial diversity may be linked to metabolic selection, which enriches specific functional bacteria while reducing overall diversity. Furthermore, the use of a single carbon source in synthetic wastewater also contributes to this effect (Hu et al., 2023). The Venn diagram illustrates changes in the main functional microorganisms, with shared OTUs between S1, S2, S3, and Seed accounting for 74.67 %, 69.76 %, and 75.82 % of total OTUs, respectively. The shared OTUs between S2 and S3 with S1 accounted for 77.54 % and 70.45 % of total OTUs, respectively, indicating that carrier addition influenced the microbial community composition (Fig. 7b).

Table 3
Interfacial free energy of interaction surface between sludge, zeolite, and attapulgite (mJ/m^2).

System	ΔG_{adh}^{LW}	ΔG_{adh}^{AB}	ΔG_{adh}
Zeolite-sludge	−1.39	−11.01	−12.40
Attapulgite-sludge	−3.14	0.06	−3.08

3.5.2. Microbial community structure and composition

The distribution and relative abundance of significant microorganisms at the phylum, class, and genus levels were examined to gain a better understanding of the impacts of carrier addition on the structure and composition of bacteria. At the phylum level, the predominant phylum groups observed in S1, S2, and S3 were consistent with those in the seed, although their relative abundances varied (Fig. 8a). The dominant phyla across S1–3 and the seed comprised Proteobacteria (27.2 %–42.6 %), Chloroflexi (18.2 %–24.2 %), Bacteroidota (14.8 %–20.1 %), Patescibacteria (7.3 %–12.2 %), and Acidobacteriota (4.3 %–9.1 %). Proteobacteria emerged as the most abundant phylum in sludge, a common observation in WWTPs (Bedoya et al., 2020). Furthermore, Planctomycetota, Chloroflexi, and Acidobacteriota are also found in WWTPs (Fujii et al., 2022). The relative abundance of Bacteroidota dropped from 18.2 % to 14.8 % in sample S2, while the relative abundance of Patescibacteria increased significantly from 27.2 % to 42.6 %. Chloroflexi contribute significantly to the availability of substrates for other microbes' metabolisms by breaking down carbohydrates (Fan et al., 2022). The enrichment of Proteobacteria aids in resisting adverse external environmental changes and maintaining denitrification stability (Li et al., 2022). Complex organic materials present in the influent, such as proteins and lipids, are easily broken down into simpler substances by Proteobacteria and Bacteroidota (Begmatov et al., 2022). This function is crucial for improving COD consumption efficiency and eliminating both N and P.

The leading species found in samples S1, S2, and S3 at the class level closely reflect those found in the seed, as shown in Fig. 8b. Across the four samples, Gammaproteobacteria (18.7 %–34.3 %), Anaerolineae (15.4 %–17.9 %), Bacteroidia (10.8 %–16.0 %), and Alphaproteobacteria (6.7 %–9.0 %) were identified as the primary dominant classes. While the relative abundance of Alphaproteobacteria in S2 stayed largely unchanged, the relative abundance of Gammaproteobacteria grew dramatically, rising from 18.7 % to 34.3 %. Microorganisms linked to N and P removal processes in WWTPs are commonly identified as Gammaproteobacteria and Alphaproteobacteria (Gu et al., 2022). Gammaproteobacteria are abundant in oligotrophic settings, and their relative abundance was significantly higher in S1–3 than in the seed. Furthermore, it has been documented that Gammaproteobacteria are capable of performing P removal and denitrification processes (Zeng et al., 2016). A more thorough study based on the top 50 prevalent taxa was presented in Fig. 8c and Table S6, revealing specific variations within the microbial communities. In the seed activated sludge, the dominant genera included *Candidatus_Competibacter* (5.76 %), *Saccharimonadales* (5.42 %), *Candidatus_Accumulibacter* (1.42 %), *Terrimonas* (2.87 %), and *Saprospiraceae* (4.01 %). Only 66.7 % of the total was accounted for by the relative abundances of the top 50 prolific taxa. Comparing the relative abundances of *Candidatus_Competibacter* and *Candidatus_Accumulibacter* to the seeding sludge, there were notable increases. Specifically, *Candidatus_Competibacter* increased to 9.68 %, 13.18 %, and 10.46 % in samples S1, S2, and S3 respectively, while *Candidatus_Accumulibacter* increased to 2.82 %, 4.23 %, and 4.66 % in the same samples. *Candidatus_Competibacter*, recognized as typical GAOs (glycogen-accumulating organisms), assumes a pivotal role in reducing nitrate to nitrite within the EBPR (enhanced biological phosphorus removal) system (Chen et al., 2024). Endogenous denitrification serves as the primary pathway for nitrogen removal, while denitrifying phosphorus removal is essential for sustaining low phosphorus concentrations in the effluent (Wang et al., 2019). Rubio-Rincon et al. proposed synergistic effects between *Candidatus_Competibacter* and *Candidatus_Accumulibacter*, whereby GAOs aid in the reduction of nitrate to nitrite, thereby bolstering the anoxic activity of PAOs (phosphorus-accumulating organisms) (Rubio-Rincón et al., 2017). Utilizing nitrite as an electron acceptor presents a more sustainable approach to simultaneously remove N and P. With GAOs/PAOs values ranging from 3 to 11,

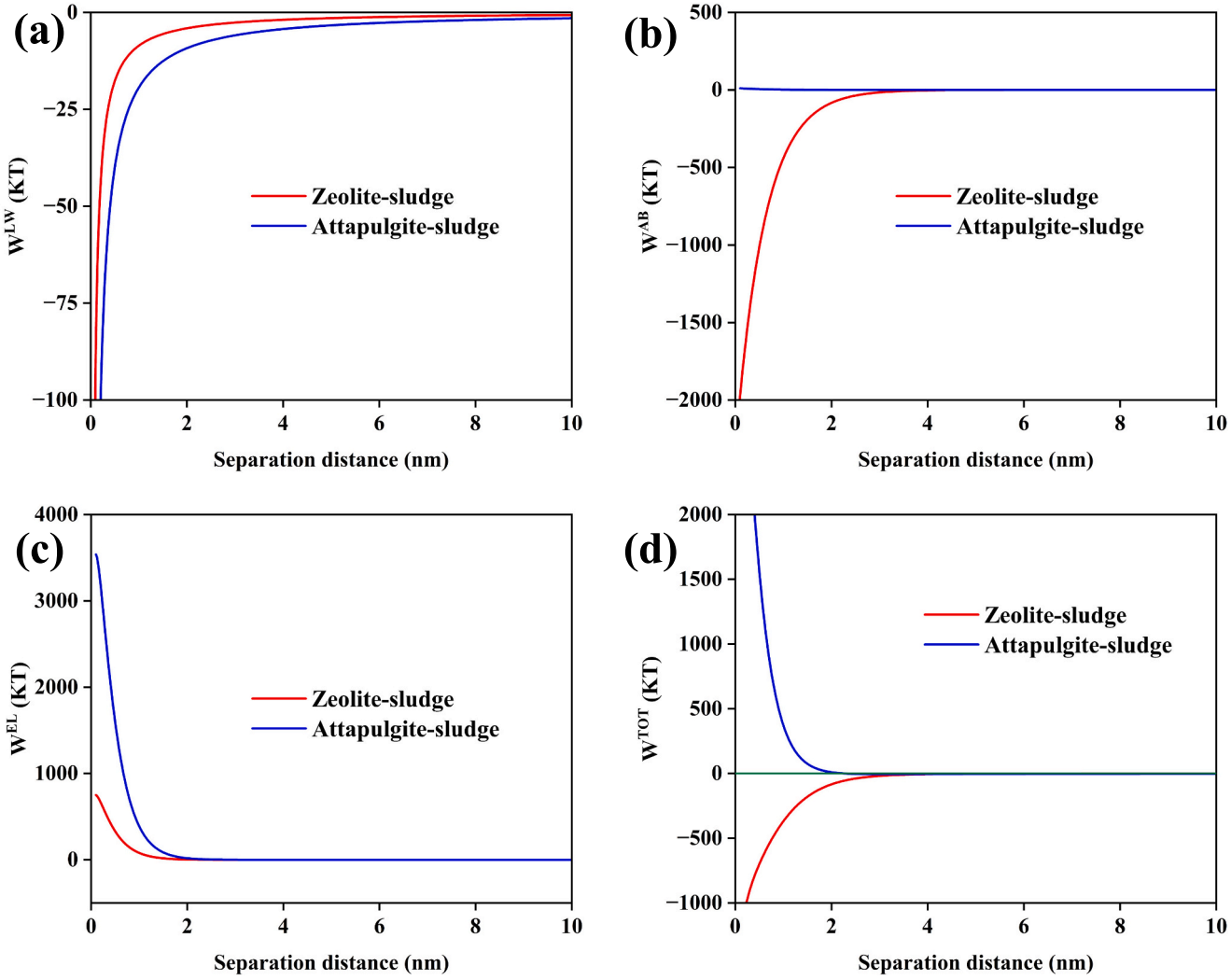

Fig. 6. The extended DLVO interaction energy profiles for Zeolite-sludge and Attapulgite-sludge, (a) van der Waals energy (W^{LW}), (b) acid-base interaction energy (W^{AB}), (c) electrical double layer energy (W^{EL}), and (d) total interaction free energy (W^{TOT}).

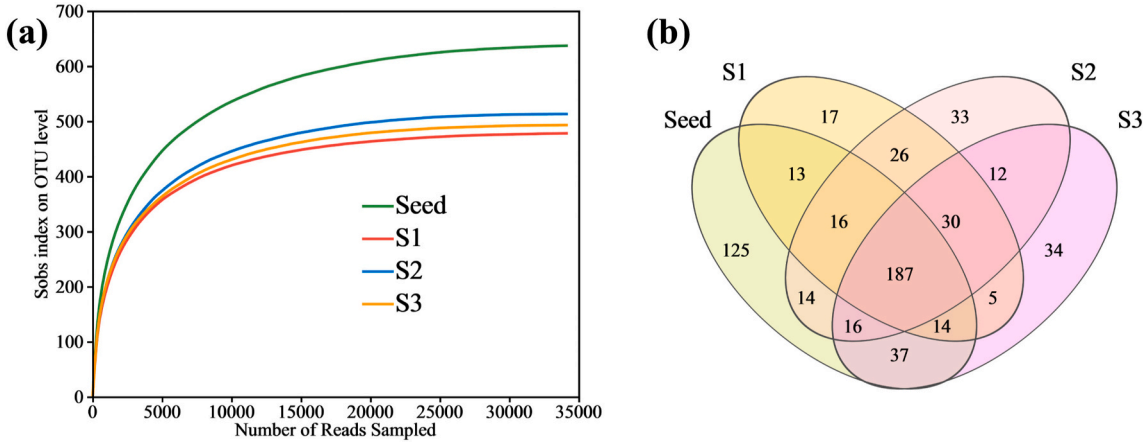

Fig. 7. Differences in diversities and microbial community structure: (a) Rarefaction curves for OTUs; (b) Venn diagram of samples.

Gao et al. achieved high removal rates of TN and total TP in an AOA system with *Candidatus_Competibacter* as the dominating genus (Gao et al., 2022). In this study, the main AOB detected were *Ellin6067* and *norank_f_NS9_marine_group*. Over time, *norank_f_NS9_marine_group* emerged as the dominant species, with relative abundances of 1.94 %, 2.52 %, and 2.92 % in S1, S2, and S3, respectively, while *Ellin6067* decreased in abundance. Differences in mass transfer between systems likely influenced AOB enrichment. NOB showed a decreasing trend, with *Nitrospira* abundances of 0.87 %, 0.43 %, and 0.62 %, respectively. The abundance of DNB in the three reactors reached in S1, S2, and S3,

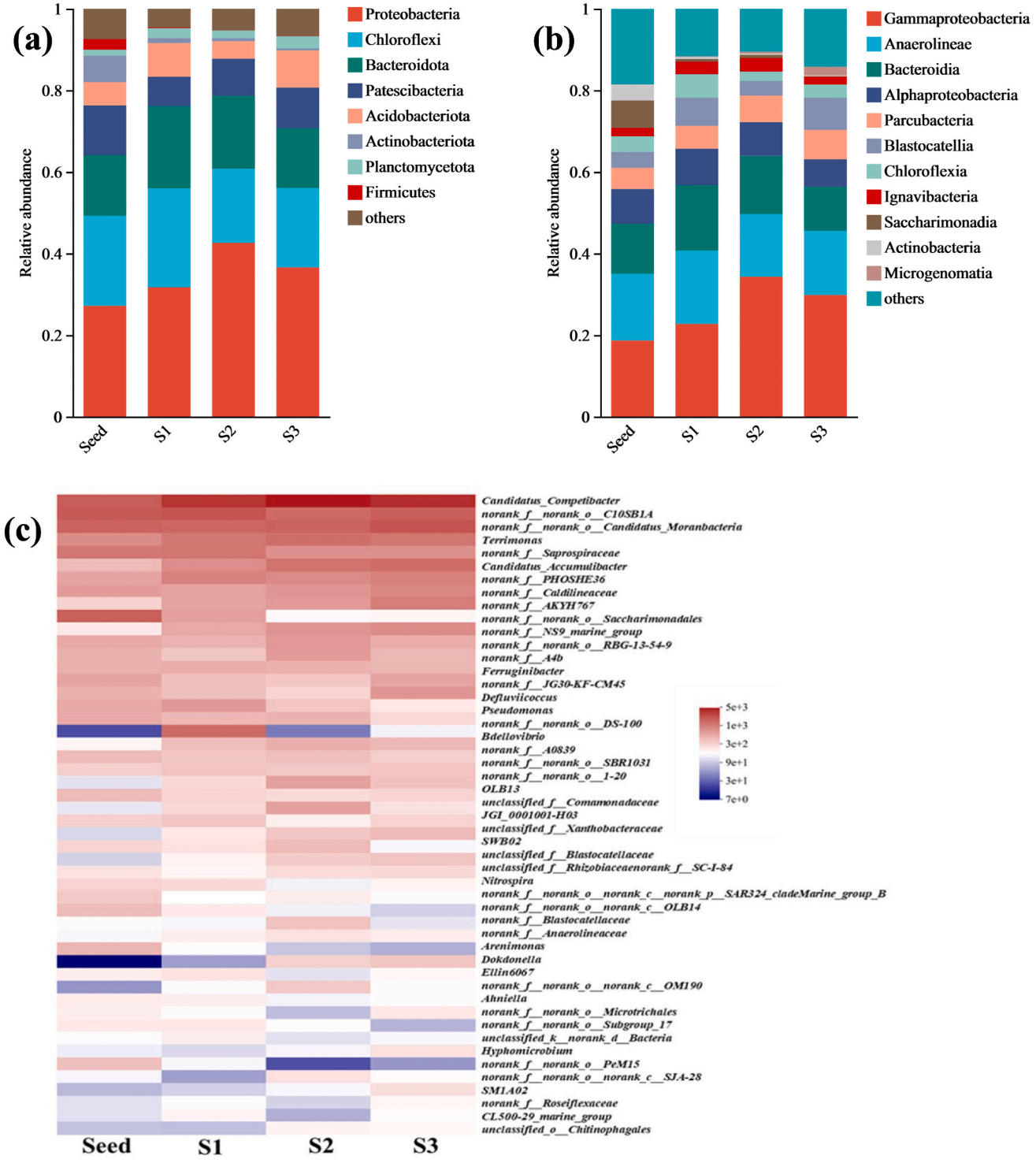

Fig. 8. Microbial compositions of samples: (a) phylum level; (b) class level; and (c) heatmap of the top 50 genera.

respectively. DNB was detected in all reactors, with abundances of 12.33 %, 15.43 %, and 12.63 % in S1, S2, and S3, respectively. Notably, *norank_f_A4b*, *Terrimonas*, and *Ferruginibacter* were particularly advantageous in these systems. *Terrimonas* abundances increased to 3.95 %, 4.4 %, and 4.06 % in S1, S2, and S3, respectively. Despite their slow growth, these denitrifying bacteria play a crucial role in nitrogen removal within the system. In summary, as the reactor operates and becomes established, more microorganisms related to nitrogen and phosphorus removal can flourish in the system. Conversely, microorganisms unable to adapt to the system conditions are gradually phased out, leading to distinct differences in microbial community structure over time (Fig. S5).

3.6. Prospects and challenges

Incorporating powder carriers into activated sludge systems enhances sedimentation performance and bolsters resilience against hydraulic impacts. For instance, in a sewage treatment plant with a capacity of 20,000 m^3/d, annual powder carriers procurement costs amount to 33,208.39 $, with an additional 3699.60 $ annually for

operating costs related to carrier addition (Wang et al., 2023a). This approach results in annual savings of 80,422.28 $ on phosphorus removal agents and 110,369.64 $ on sodium acetate (which lowers TN and TP) (Yang et al., 2024b). In practical applications, hydraulic cyclones can recover carriers, further reducing procurement costs and operational expenses on a larger scale. Despite the need for acquiring new equipment such as hydrocyclone separators, these costs are considerably lower than ongoing operational expenses.

However, several considerations require further evaluation: developing efficient hydrocyclones to enhance carriers recovery, assessing the impact of powder carrier addition on subsequent sludge treatment and disposal despite its inert nature, and optimizing operational parameters (including SRT, HRT, DO, etc.) to better align with practical application requirements.

4. Conclusion

Incorporating zeolite and attapulgite as powdered carriers into wastewater treatment systems significantly enhances their effectiveness. This addition increases the concentration of MLVSS, which in turn boosts microbial activity and improves sludge settling performance. Additionally, these carriers alter the microbial community structure, enriching populations of key microorganisms such as *Candidatus_Accumulibacter* and *Candidatus_Competibacter*, which are crucial for effective N and P removal. The carriers also promote the production of EPS by microorganisms, enhancing their ability to aggregate and form biofilms. From a thermodynamic perspective, surface free energy analyses indicate that sludge microorganisms exhibit a higher affinity for adhesion to zeolite carriers. These materials are not only effective and biocompatible but also environmentally friendly and readily available, thereby significantly improving the performance of WWTP.

CRediT authorship contribution statement

Yi Yang: Writing – review & editing, Writing – original draft, Visualization, Investigation, Data curation, Conceptualization. **Yuting Zhu:** Investigation, Conceptualization. **Defu Gan:** Investigation, Conceptualization. **Xiang Cai:** Investigation, Conceptualization. **Xiaodi Li:** Investigation, Conceptualization. **Xinchao Liu:** Investigation, Conceptualization. **Siqing Xia:** Supervision, Methodology, Investigation, Funding acquisition, Conceptualization.

Declaration of competing interest

The authors declare no competing interests.

Data availability

No data was used for the research described in the article.

Acknowledgments

This work was supported by the National Key Project of Research and Development Plan of China (2021YFC3201300).

Appendix A. Supplementary data

Supplementary data to this article can be found online at https://doi.org/10.1016/j.scitotenv.2024.175812.

References

Abu Bakar, S.N.H., Abu Hasan, H., Mohammad, A.W., Abdullah, S.R.S., Haan, T.Y., Ngteni, R., Yusof, K.M.M., 2018. A review of moving-bed biofilm reactor technology for palm oil mill effluent treatment. J. Clean. Prod. 171, 1532–1545.

APHA, 2012. Standard Methods for the Examination of Water and Wastewater. American Public Health Association, Washington. DC.

Arabgol, R., Vanrolleghem, P.A., Delatolla, R., 2022. Influence of MBBR carrier geometrical properties and biofilm thickness restraint on biofilm properties, effluent particle size distribution, settling velocity distribution, and settling behaviour. J. Environ. Sci. 122, 138–149.

Aslam, Z., Alam, P., Islam, R., Khan, A.H., Samaraweera, H., Hussain, A., Zargar, T.I., 2024. Recent developments in moving bed biofilm reactor (MBBR) for the treatment of phenolic wastewater -a review. J. Taiwan Inst. Chem. Eng. 105517.

Bedoya, K., Hoyos, O., Zurek, E., Cabarcas, F., Alzate, J.F., 2020. Annual microbial community dynamics in a full-scale anaerobic sludge digester from a wastewater treatment plant in Colombia. Sci. Total Environ. 726, 138479.

Begmatov, S., Dorofeev, A.G., Kadnikov, V.V., Beletsky, A.V., Pimenov, N.V., Ravin, N.V., Mardanov, A.V., 2022. The structure of microbial communities of activated sludge of large-scale wastewater treatment plants in the city of Moscow. Sci. Report. 12 (1).

Boks, N.P., Norde, W., van der Mei, H.C., Busscher, H.J., 2008. Forces involved in bacterial adhesion to hydrophilic and hydrophobic surfaces. Microbiology 154 (10), 3122–3133.

Bos, R., van der Mei, H.C., Busscher, H.J., 1999. Physico-chemistry of initial microbial adhesive interactions - its mechanisms and methods for study. FEMS Microbiol. Rev. 23 (2), 179–230.

Chen, J., Zeng, J., He, Y., Sun, S., Wu, H., Zhou, Y., Chen, Z., Wang, J., Chen, H., 2023. Insights into a novel nitrogen removal process based on simultaneous anammox and denitrification (SAD) following nitritation with in-situ NOB elimination. J. Environ. Sci. 125, 160–170.

Chen, R., Ren, L.-F., Shao, J., He, Y., Zhang, X., 2017. Changes in degrading ability, populations and metabolism of microbes in activated sludge in the treatment of phenol wastewater. RSC Adv. 7 (83), 52841–52851.

Chen, R., Guo, W., Li, L., Wang, H., Wang, B., Hu, X., Ji, B., Zhou, D., Lyu, W., 2024. Aerobic granulation in a continuous-flow simultaneous nitrification, endogenous denitrification, and phosphorus removal system fed with low-strength wastewater: granulation mechanism and microbial succession. Chem. Eng. J. 487, 150598.

Collivignarelli, M.C., Abbà, A., Bertanza, G., 2019. Oxygen transfer improvement in MBBR process. Environ. Sci. Pollut. Res. 26 (11), 10727–10737.

Fan, Q., Fan, X., Fu, P., Sun, Y., Li, Y., Long, S., Guo, T., Zheng, L., Yang, K., Hua, D., 2022. Microbial community evolution, interaction, and functional genes prediction during anaerobic digestion in the presence of refractory organics. J. Environ. Chem. Eng. 10 (3), 107789.

Fan, X., Zhu, S.-S., Zhang, X.-X., Ren, H.-Q., Huang, H., 2021. Revisiting the microscopic processes of biofilm formation on organic carriers: a study under variational shear stresses. ACS Appl. Bio Mater. 4 (7), 5529–5541.

Fujii, N., Kuroda, K., Narihiro, T., Aoi, Y., Ozaki, N., Ohashi, A., Kindaichi, T., 2022. Metabolic potential of the superphylum patescibacteria reconstructed from activated sludge samples from a municipal wastewater treatment plant. Microbes Environ. 37 (3).

Gao, X., Xue, X., Li, L., Peng, Y., Yao, X., Zhang, J., Liu, W., 2022. Balance nitrogen and phosphorus efficient removal under carbon limitation in pilot-scale demonstration of a novel anaerobic/aerobic/anoxic process. Water Res. 223, 118991.

Gu, Y., Li, B., Zhong, X., Liu, C., Ma, B., 2022. Bacterial community composition and function in a tropical municipal wastewater treatment plant. Water 14 (10), 1537.

Gupta, B., Gupta, A.K., Ghosal, P.S., Lal, S., Saidulu, D., Srivastava, A., Upadhyay, M., 2022. Recent advances in application of moving bed biofilm reactor for wastewater treatment: insights into critical operational parameters, modifications, field-scale performance, and sustainable aspects. J. Environ. Chem. Eng. 10 (3), 107742.

Hasan, M.N., Altaf, M.M., Khan, N.A., Khan, A.H., Khan, A.A., Ahmed, S., Kumar, P.S., Naushad, M., Rajapaksha, A.U., Iqbal, J., Tirth, V., Islam, S., 2021. Recent technologies for nutrient removal and recovery from wastewaters: a review. Chemosphere 277, 130328.

Hu, K., Li, W., Wang, Y., Wang, B., Mu, H., Ren, S., Zeng, K., Zhu, H., Liang, J., Wang, Y. e., Xiao, J., 2023. Novel biological nitrogen removal process for the treatment of wastewater with low carbon to nitrogen ratio: a review. Journal of Water Process Engineering. 53, 103673.

Iritani, E., Nishikawa, M., Katagiri, N., Kawasaki, K., 2015. Synergy effect of ultrasonication and salt addition on settling behaviors of activated sludge. Sep. Purif. Technol. 144, 177–185.

Jiang, Y., Khan, A., Huang, H., Tian, Y., Yu, X., Xu, Q., Mou, L., Lv, J., Zhang, P., Liu, P., Deng, L., Li, X., 2019. Using nano-attapulgite clay compounded hydrophilic urethane foams (AT/HUFs) as biofilm support enhances oil-refinery wastewater treatment in a biofilm membrane bioreactor. Sci. Total Environ. 646, 606–617.

Lago, A., Rocha, V., Barros, O., Silva, B., Tavares, T., 2024. Bacterial biofilm attachment to sustainable carriers as a clean-up strategy for wastewater treatment: a review. Journal of Water Process Engineering. 63, 105368.

Li, J., Zheng, L., Ye, C., Zhou, Z., Ni, B., Zhang, X., Liu, H., 2022. Unveiling organic loading shock-resistant mechanism in a pilot-scale moving bed biofilm reactor-assisted dual-anaerobic-anoxic/oxic system for effective municipal wastewater treatment. Bioresour. Technol. 347, 126339.

Li, X., Feng, Y., Zhang, K., Zhou, J., Sun, J., Rong, K., Liu, S., 2023. Composite carrier enhanced bacterial adhesion and nitrogen removal in partial nitrification/anammox process. Sci. Total Environ. 868, 161659.

Ma, J., Ji, Y., Fu, Z., Yan, X., Xu, P., Li, J., Liu, L., Bi, P., Zhu, L., Xu, B., He, Q., 2023. Performance of anaerobic/oxic/anoxic simultaneous nitrification, denitrification and phosphorus removal system overwhelmingly dominated by Candidatus_Competibacter: effect of aeration time. Bioresour. Technol. 384, 129312.

Matheus, M.C., Ekenberg, M., Bassin, J.P., Dezotti, M.W.C., Piculell, M., 2021. High loaded moving bed biofilm reactors treating pulp & paper industry wastewater: effect of hydraulic retention time, filling degree and nutrients availability on performance, biomass fractions and nutrients utilization. J. Environ. Chem. Eng. 9 (1), 104944.

Mu, Y., Wan, L., Liang, Z., Yang, D., Han, H., Yi, J., Dai, X., 2023. Enhanced biological phosphorus removal by high concentration powder carrier bio-fluidized bed (HPB): phosphorus distribution, cyclone separation, and metagenomics. Chemosphere 337, 139353.

Osama, A., Kinnawy, M.A., Moussa, M.S., Riechelmann, C., Hosney, H., 2023. Mathematical modelling and comparative analysis of treatment technologies for upgrading wastewater treatment plants: a case study of biofilm reactors in El-Gouna, Egypt. Environ. Res. 238, 117008.

Osmani, S.A., Rajpal, A., Kazmi, A.A., 2021. Upgradation of conventional MBBR into aerobic/anoxic/aerobic configuration: a case study of carbon and nitrogen removal based sewage treatment plant. Journal of Water Process Engineering. 40, 101921.

Park, S.-J., Oh, J.-W., Yoon, T.-I., 2003. The role of powdered zeolite and activated carbon carriers on nitrification in activated sludge with inhibitory materials. Process Biochem. 39 (2), 211–219.

Powley, H.R., Dürr, H.H., Lima, A.T., Krom, M.D., Van Cappellen, P., 2016. Direct discharges of domestic wastewater are a major source of phosphorus and nitrogen to the Mediterranean Sea. Environ. Sci. Technol. 50 (16), 8722–8730.

Qu, J., Dai, X., Hong-Ying, H., Huang, X., Chen, Z., Li, T., Cao, Y., Daigger, G.T., 2022. Emerging trends and prospects for municipal wastewater management in China. Acs Es&T Engineering. 2 (3), 323–336.

Rubio-Rincón, F.J., Lopez-Vazquez, C.M., Welles, L., van Loosdrecht, M.C.M., Brdjanovic, D., 2017. Cooperation between Candidatus Competibacter and Candidatus Accumulibacter clade I, in denitrification and phosphate removal processes. Water Res. 120, 156–164.

Ruprecht, J.E., Birrer, S.C., Dafforn, K.A., Mitrovic, S.M., Crane, S.L., Johnston, E.L., Wemheuer, F., Navarro, A., Harrison, A.J., Turner, I.L., Glamore, W.C., 2021. Wastewater effluents cause microbial community shifts and change trophic status. Water Res. 200, 117206.

Sakaveli, F., Petala, M., Tsiridis, V., Karas, P.A., Karpouzas, D.G., Darakas, E., 2023. Effect of attapulgite on anaerobic digestion of primary sludge and downstream valorization of produced biosolids. Renew. Energy 217, 119211.

Sun, Y., Chen, Z., Wu, G., Wu, Q., Zhang, F., Niu, Z., Hu, H.-Y., 2016. Characteristics of water quality of municipal wastewater treatment plants in China: implications for resources utilization and management. J. Clean. Prod. 131, 1–9.

Tang, Y., Dai, X., Dong, B., Guo, Y., Dai, L., 2020. Humification in extracellular polymeric substances (EPS) dominates methane release and EPS reconstruction during the sludge stabilization of high-solid anaerobic digestion. Water Res. 175, 115686.

Wang, C., Lu, B., Chen, H., Chen, H., Li, T., Lu, W., Chai, X., 2023a. Strengthen high-loading operation of wastewater treatment plants by composite micron powder carrier: microscale control of carbon, nitrogen, and sulfur metabolic pathways. Sci. Total Environ. 904, 166593.

Wang, H., Chen, Y., Liu, X., Xu, H., Yang, D., Hua, Y., Dai, X., 2024a. Diatomite powder carrier improved nitrogen and phosphorus removal from real municipal wastewater: insights into micro-granule formation and enhancement mechanism. Chem. Eng. J. 484, 149482.

Wang, H., Xu, H., Liu, X., Hua, Y., Yang, D., Dai, X., 2024b. A novel process based on powder carriers demonstrates robustness in nitrogen and phosphorus removal from real municipal wastewater. Water Res. 251, 121149.

Wang, K., Zhou, C., Zhou, H., Jiang, M., Chen, G., Wang, C., Zhang, Z., Zhao, X., Jiang, L.-M., Zhou, Z., 2023b. Comparison on biological nutrient removal and microbial community between full-scale anaerobic/anoxic/aerobic process and its upgrading processes. Bioresour. Technol. 374, 128757.

Wang, R., Wang, X., Deng, C., Chen, Z., Chen, Y., Feng, X., Zhong, Z., 2020. Partial nitritation performance and microbial community in sequencing batch biofilm reactor filled with zeolite under organics oppression and its recovery strategy. Bioresour. Technol. 305, 123031.

Wang, X., Zhao, J., Yu, D., Du, S., Yuan, M., Zhen, J., 2019. Evaluating the potential for sustaining mainstream anammox by endogenous partial denitrification and phosphorus removal for energy-efficient wastewater treatment. Bioresour. Technol. 284, 302–314.

Wolff, D., Helmholz, L., Castronovo, S., Ghattas, A.-K., Ternes, T.A., Wick, A., 2021. Micropollutant transformation and taxonomic composition in hybrid MBBR – a comparison of carrier-attached biofilm and suspended sludge. Water Res. 202, 117441.

Xiao, K., Li, N., Yang, C., Zhu, Y., Yu, Z., Yu, W., Liang, S., Hou, H., Liu, B., Hu, J., Yang, J., 2021. Deciphering the impacts of composition of extracellular polymeric substances on sludge dewaterability: an often overlooked role of amino acids. Chemosphere 284, 131297.

Xu, J., Yu, H.-q., Li, X.-y., 2016. Probing the contribution of extracellular polymeric substance fractions to activated-sludge bioflocculation using particle image velocimetry in combination with extended DLVO analysis. Chem. Eng. J. 303, 627–635.

Yang, N., Zhang, Y., Yang, S., 2024a. Structural characteristics of organics released from sludge pretreatment and their performance in the synthesis of biomass plastics. Chem. Eng. J. 490, 151391.

Yang, Y., Bai, W., Gan, D., Zhu, Y., Li, X., Liang, C., Xia, S., 2024b. A practical study on the near-zero discharge of rainwater and the collaborative treatment and regeneration of rainwater and sewage. Sci. Total Environ. 934, 173137.

Zeng, W., Zhang, J., Wang, A., Peng, Y., 2016. Denitrifying phosphorus removal from municipal wastewater and dynamics of “Candidatus Accumulibacter” and denitrifying bacteria based on genes of ppk1, narG, nirS and nirK. Bioresour. Technol. 207, 322–331.

Zhang, H., Jia, Y., Khanal, S.K., Lu, H., Fang, H., Zhao, Q., 2018. Understanding the role of extracellular polymeric substances on ciprofloxacin adsorption in aerobic sludge, anaerobic sludge, and sulfate-reducing bacteria sludge systems. Environ. Sci. Technol. 52 (11), 6476–6486.

Zhang, X., Zhou, X., Xi, H., Sun, J., Liang, X., Wei, J., Xiao, X., Liu, Z., Li, S., Liang, Z., Chen, Y., Wu, Z., 2019. Interpretation of adhesion behaviors between bacteria and modified basalt fiber by surface thermodynamics and extended DLVO theory. Colloids Surf. B: Biointerfaces 177, 454–461.

Zhang, Y., Li, M., Zhang, G., Liu, W., Xu, J., Tian, Y., Wang, Y., Xie, X., Peng, Z., Li, A., Zhang, R., Wu, D., Xie, X., 2023. Efficient treatment of the starch wastewater by enhanced flocculation–coagulation of environmentally benign materials. Sep. Purif. Technol. 307, 122788.

Zhao, Y., Zhu, S., Fan, X., Zhang, X., Ren, H., Huang, H., 2022. Precise portrayal of microscopic processes of wastewater biofilm formation: taking SiO2 as the model carrier. Sci. Total Environ. 849, 157776.